Phase-sensitive QPSK channel phase quantization by amplifying the fourth-harmonic idler using counter-propagating Brillouin amplification

Ahmed Almaiman[a,*], Yinwen Cao[a], Amirhossein Mohajerin-Ariaei[a], Morteza Ziyadi[a], Peicheng Liao[a], Changjing Bao[a], Fatemeh Alishahi[a], Ahmad Fallahpour[a], Bishara Shamee[a], Youichi Akasaka[b], Tadashi Ikeuchi[b], Steven Wilkinson[c], Joseph D. Touch[d], Moshe Tur[e], Alan E. Willner[a]

[a] *Department of Electrical Engineering, University of Southern California, Los Angeles, California 90089, USA*
[b] *Fujitsu Laboratories of America, 2801 Telecom Parkway, Richardson, Texas 75082, USA*
[c] *Raytheon Company, El Segundo, CA 90245, USA*
[d] *Manhattan Beach, California 90266, USA*
[e] *School of Electrical Engineering, Tel Aviv University, Ramat Aviv 69978, Israel*

Abstract

We experimentally demonstrate all-optical phase-sensitive quantization of a 10-20 Gbaud quadrature phase-shift keying (QPSK) signal's phase without an active phase-locked loop (PLL) by utilizing Brillouin amplification (BA) to amplify the fourth-harmonic idler without path separation, allowing the pump, signal, third-harmonic idler and amplified fourth-harmonic idler to remain synchronized in the phase. We observe up to 65% reduction in phase noise and 4.6 dB gain at a bit-error rate (BER) of 10^{-4} over 36 minutes of continues operation.

Keywords: All-optical phase regeneration

Phase-sensitive amplification

Wavelength conversion

Four-wave mixing

*Corresponding author
Email address: Almaiman@usc.edu (Ahmed Almaiman)

1. Introduction

Phase-dependent data modulation formats have gained interest in optical communication systems due to their relative increase in receiver sensitivity, tolerance to nonlinear effects, and spectral efficiency [1]. One challenge for the phase modulated signals is to reduce the accumulated phase noise (ϕ_{noise}) that moves data constellation points away from the ideal symbol location [2].

Phase-modulated data channels may benefit from all-optical regeneration to avoid the optical-electrical-optical conversions [3]. A potentially promising technique to reduce a QPSK signal's phase noise is to combine the signal with its conjugate third-harmonic (S^{3*}) using phase-sensitive (PS) processes [4, 5]. For example, PS-based QPSK phase quantization takes place in a highly nonlinear fiber (HNLF) with four-wave mixing (FWM), when two pumps are used to mix and add the S^{3*} to S. This "squeezes" the part of the signal that has a different phase from the ideal QPSK phase states, thereby quantizing the phase of the signal.

Previously reported approaches for optical phase quantization of QPSK signals include: (i) the amplification of the fourth-harmonic idler using injection-locked laser and phase-locked loop (PLL) for stabilization [5, 6, 7], (ii) wave mixing of a signal with its delayed conjugate, which alters the original data pattern mapping [8], and (iii) the use of cross-phase modulation and frequency comb lines [9].

PS-regeneration for binary phase-shift keying (BPSK) signals has been realized without a PLL by amplifying the idler with the signal's second harmonic using Brillouin amplification (BA) [10]. In this paper, we use that principle to quantize a QPSK signal's phase without a PLL by applying the following changes [11]: (i) create the signal's third- and fourth-harmonic idlers in the first FWM stage by sending the signal and pump with higher power levels, (ii) compensate for the delay between the signal and higher-order harmonics that is induced by dispersion walk-off in the BA gain medium, (iii) amplify the weak signal's fourth-harmonic idler with $\sim$ 40 dB BA gain [12, 13, 14], and (iv) mix

the pump and amplified fourth-harmonic idler to add the signal to its S^{3*} in a second FWM stage. We send a 10-20 Gbaud QPSK signal loaded with phase noise to the system and observe up to a 65% reduction in the phase noise variance and 4.6 dB OSNR improvement at a BER of 10^{-4}. In addition, the system shows operation without a PLL for 36 minutes.

Section 2 explains the theory of all-optically quantizing the QPSK signal's phase. Section 3 explains the concept of quantizing the QPSK phase without a PLL using Brillouin amplification. Section 4 describes the experimental setup. Section 5 presents the experimental results of quantizing the phase of a 10-20 Gbaud QPSK channel along with the effect of tuning the BA's frequency shifter. Section 6 presents the conclusions.

2. Theory

Quantizing the phase of a QPSK signal can be done by adding the signal to its conjugate third-harmonic as in Equation (1) [4]:

$$S_{\text{out}} \propto e^{(j\phi_{\text{in}})} + \frac{1}{3}e^{(-j3\phi_{\text{in}})} \tag{1}$$

Where S_{out} is the phase quantized signal and ϕ_{in} is the input signal's phase. A simulation of quantizing the phase of a QPSK signal loaded with phase noise is shown in Fig. 1.

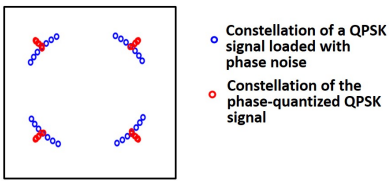

Fig. 1. Constellations of an input QPSK signal with phase noise, and the phase quantization output (simulation).

3. Concept

The concept of an all-optical QPSK phase quantizer without a PLL using Brillouin amplification is shown in Fig. 2. A QPSK signal ($S \propto e^{(j\phi_S)}$) degraded

with ϕ_{noise} is combined with a CW pump ($P \propto e^{(j\phi_{pump})}$) and sent into HNLF_1 to generate the second-, third-, and fourth-harmonic idlers, where ϕ_{S} is the input signal's phase and ϕ_{pump} is the pump laser's phase noise. The idlers will be created in HNLF_1 through FWM as:

$$idler_{2\phi_S} \propto P^* S^2 \propto e^{(-j\phi_{pump})} e^{(j2\phi_S)} \tag{2}$$

$$idler_{3\phi_S} \propto (P^*)^2 S^3 \propto e^{(-2j\phi_{pump})} e^{(j3\phi_S)} \tag{3}$$

$$idler_{4\phi_S} \propto (P^*)^3 S^4 \propto e^{(-3j\phi_{pump})} e^{(j4\phi_S)} \tag{4}$$

$\text{Idler}_{4\phi_{\text{S}}}$ is a continuous wave (CW) because $4\phi_{\text{S}}$=$4\phi_{\text{data}}$+$4\phi_{\text{noise}}$ and $\phi_{\text{data}} \in$ [$\pi/4$, $3\pi/4$, $5\pi/4$, $7\pi/4$]. So, $4\phi_{\text{data}} \in$ [π,π,π,π] and $4\phi_{\text{S}} \propto 4\phi_{\text{data}}$+$4\phi_{\text{noise}}$ π + $4\phi_{\text{noise}}$ which can be interpreted as a CW wave with four times the phase noise.

Next, in a Liquid Crystal on Silicon (LCoS) programmable filter, $\text{idler}_{2\phi_{\text{S}}}$ is blocked and S is slightly attenuated to adjust the amplitude levels and apply the relative 1/3 scaling factor (see eqn. 1) that will be needed in the following mixing stage. Also, the delay between S and idlers due to dispersion walk-off in the forthcoming BA gain medium is compensated.

Then, $\text{idler}_{4\phi_{\text{S}}}$ gets amplified in the single-mode fiber (SMF-28) with Brillouin gain (G_{B}) using a counter-propagating BA pump. BA depends on the frequency-locking between the pump and probe (the probe is $\text{idler}_{4\phi_{\text{S}}}$ in our case) [12, 13, 14]. To ensure frequency-locking between $\text{idler}_{4\phi_{\text{S}}}$ and the BA pump, the BA pump is generated by tapping $\text{idler}_{4\phi_{\text{S}}}$ after HNLF_1 and sending it to a slave laser (the blue area in Fig. 2). The slave laser gives a frequency-locked CW output, which is then frequency up-shifted by ν_{B} (ν_{B}:Brillouin gain frequency shift of the medium), amplified, and sent into the SMF-28 as a counter-propagating BA pump. For SMF-28, $\nu_{\text{B}} \approx 10.8$ GHz.

At the SMF-28 output, the P, S, $\text{idler}_{3\phi_{\text{S}}}$, and $\text{idler}_{4\phi_{\text{S}}} \times \text{G}_{\text{B}}$ are boosted using an erbium-doped fiber amplifier (EDFA) and sent into HNLF_2. In HNLF_2, non-degenerate FWM mixing between the pump, $\text{idler}_{4\phi_{\text{S}}} \times \text{G}_{\text{B}}$, and $\text{idler}_{3\phi_{\text{S}}}$, creates $e^{(\text{-j}3\phi_{\text{S}})}$ at the same frequency as of the signal (ω_{S}), and S_{out} is then realized. Also, because $\text{idler}_{4\phi_{\text{S}}}$ propagates in the forward direction in the same path as

the other harmonics, its phase will relatively remain locked (i.e., synchronized) to P, S, and idler$_{3\phi_S}$ without requiring a PLL [11].

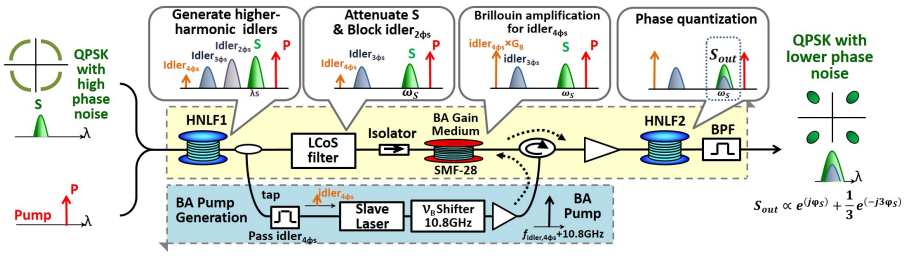

Fig. 2. The concept of QPSK channel phase quantization without a phase-locked loop using Brillouin amplification.

4. Experimental Setup

The experimental setup is depicted in Fig. 3(a). A QPSK signal is generated by modulating a laser at wavelength λ_S=1553.9 nm in an I/Q Mach-Zehnder modulator (MZM) with 2^{31}-1 pseudorandom binary sequence (PRBS) non-return-to-zero (NRZ) pulses at 10-20 Gbaud. ϕ_{noise} is loaded using a phase modulator driven by a 5.5-GHz clock source. The signal and a CW pump at λ_P=1553.1 nm are combined in a 50/50 coupler, and sent together into a 450 m HNLF$_1$. HNLF$_1$ has zero-dispersion wavelength (ZDW) at 1556 nm. Linewidths of Laser-1 and Laser-2 are less than 10 kHz, and each of the signal and pump has $\sim$ 20 dBm at HNLF$_1$ input. The measured reflected power from HNLF$_1$ at the power meter (PM$_1$) due to the stimulated Brillouin scattering (SBS) is $\sim$ +2 dBm.

The output spectrum of HNLF$_1$ is shown in Fig. 3(b). HNLF$_1$ output is sent to the LCoS programmable filter to attenuate S, block idler$_{2\phi_S}$, adjust relative phases, and compensate for the delay that will be induced by dispersion walk-off in the upcoming 500 m SMF-28. The added delay values are shown in Fig. 3(c). Afterwards, the LCoS filter output is sent to the BA gain medium (500 m SMF-28) to amplify the central carrier of idler$_{4\phi_S}$ using the counter-propagating BA pump.

The BA pump is generated in the "BA pump generation" path by selecting

idler$_{4\phi_S}$ using a band-pass filter (BPF) after the 50/50 coupler and sending it to a slave laser. The slave laser (Eblana photonics 1550-NLW) is temperature-controlled so that it locks to idler$_{4\phi_S}$ within ± 200 MHz range. The slave laser output is then frequency up-shifted in a MZM biased at null and driven by a ν_B=10.805 GHz tone. The modulator is followed by a sharp filter to passes only the upper tone. The upper tone is boosted in an EDFA and sent to the 500 m SMF-28 from its opposite end as the counter-propagating BA pump.

The BA pump EDFA is operated at ∼27 dB, and the pump power level corresponds to the operating point shown in Fig. 3(d). The SMF-28 output is shown in Fig. 3(e) before (in red) and after (in blue) amplifying idler$_{4\phi_S}$. Figure 3(f) shows the spectrum of idler$_{4\phi_S}$ after the SMF-28, which is captured using a high-resolution (10-MHz) optical spectrum analyzer (OSA). The central carrier of idler$_{4\phi_S}$ has gained G_B∼40 dB while the 5.5-GHz ϕ_{noise} spectral components are not amplified. The spectrum is captured for a 10 Gbaud NRZ signal with bandwidth extending ±10 GHz around the optical carrier, and the 5.5-GHz ϕ_{noise} tones thus reside within the signal's band. Also, in Fig. 3(f), a crosstalk tone appears at 10.8 GHz due to the BA pump leakage between port 1 and port 3 in circulator$_2$. This power leakage could fall within the signal's band if the signal's baud rate becomes greater than 10.8 GHz.

Next, P, S, idler$_{3\phi_S}$, and idler$_{4\phi_S}$×G_B are amplified in EDFA$_6$, which is set to deliver 26 dBm at HNLF$_2$ input. HNLF$_2$ has ZDW=1545 nm and the measured reflected power due to the SBS is -10 dBm at PM$_2$. The phase quantization stage output is shown in Fig. 3(g) along with the case of blocking S, to illustrate that the created $e^{(-j3\phi_S)}$ at ω_S, is optimized to be 10 dB lower than the signal (1/3 difference in magnitude). The OSNR of S_{out} is 22.3 dB (20.6 dB measured at 0.1 nm resolution). The low OSNR is caused by noise-loading in EDFA$_6$ when amplifying the relatively low power signal and idler$_{3\phi_S}$. At the output, the quantized QPSK signal is filtered and sent to an 80 Gsample/s coherent receiver.

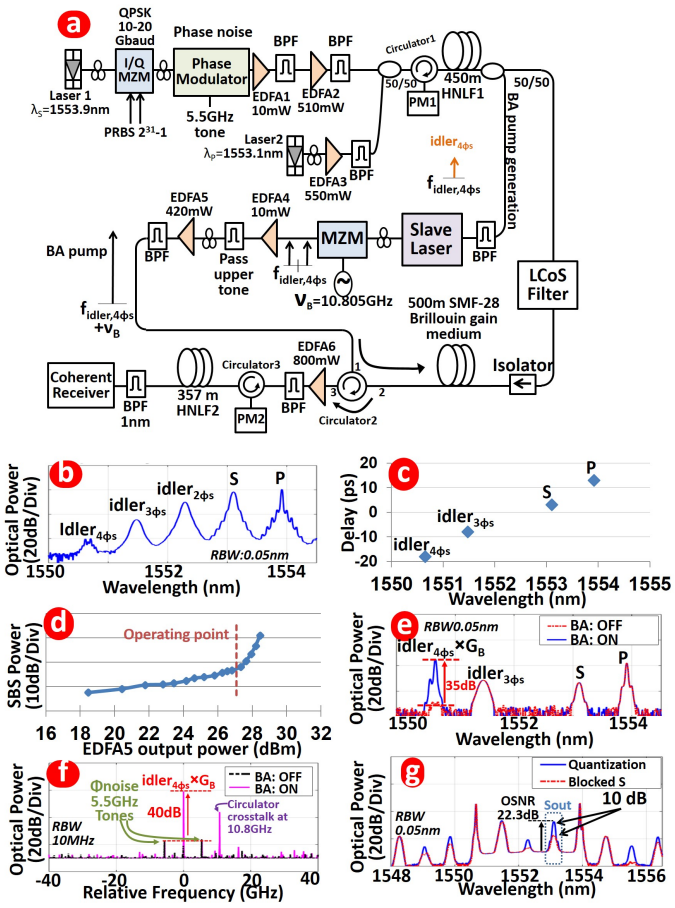

Fig. 3. (a) Experimental setup. (b) The spectrum of generated idlers after HNLF_1. (c) Applied delay in the LCoS filter to compensate for the dispersion-induced walk-off in the 500 m SMF-28 between P, S, $\text{idler}_{3\phi_S}$, and $\text{idler}_{4\phi_S}$. (d) BA operating point as a function of EDFA_5 output power. (e) Spectrum at the SMF-28 output to show the amplification on $\text{idler}_{4\phi_S}$. (f) Spectrum of the amplified $\text{idler}_{4\phi_S}$ captured using a 10-MHz resolution optical spectrum analyzer, showing that $\text{idler}_{4\phi_S}$'s central component gains 40 dB, while the 5.5-GHz ϕ_{noise} components are not amplified. (g) HNLF_2 output when the system is quantizing the phase, and when S is blocked to observe the ∼10 dB power difference between $e^{(j\phi_S)}$ and $e^{(-j3\phi_S)}$.

5. Experimental Results

Figure 4(a) depicts the constellations resulted from quantizing the phase of degraded signal with ϕ_{noise}. The phase noise levels are varied and following parameters are recorded: (i) constellation, (ii) error-vector-magnitude (EVM) (iii) phase noise variance ($\Delta\phi$), (iv) magnitude error (MagErr), and (v) the Q-factor (Q). From the noise-free (Level-5) scenarios, the system adds 1.3-dB Q-factor penalty to the 10-Gbaud signal and 2-dB penalty to the 20-Gbaud case. Fig. 4(b) shows the percentages of improvement for the figures-of-merit with respect to the input $\Delta\phi$. When the 10-Gbaud QPSK signal is transmitted, reductions of up to 65% in $\Delta\phi$ and 48% in the EVM are observed for the high phase noise scenario (corresponding to Level-1). At 20 Gbaud, the highest recorded improvements in $\Delta\phi$ and EVM are 43.9% and 30.3%, respectively. Fig. 4(c) shows the BER of the output and indicates up to a 3.4-dB improvement at a BER of 10^{-4} for the 10-Gbaud case. The BER is calculated by counting the errors of ∼500,000 bits for every point. The 20-Gbaud signal exhibits receiver sensitivity improvement of 1.8 dB at Level-3 and the improvement is 2.6 dB at Level-2. We also observe a BER floor for the 20 Gbaud Level-2 input signal, and the output follows the same error floor at a BER of 5.6×10^{-5}.

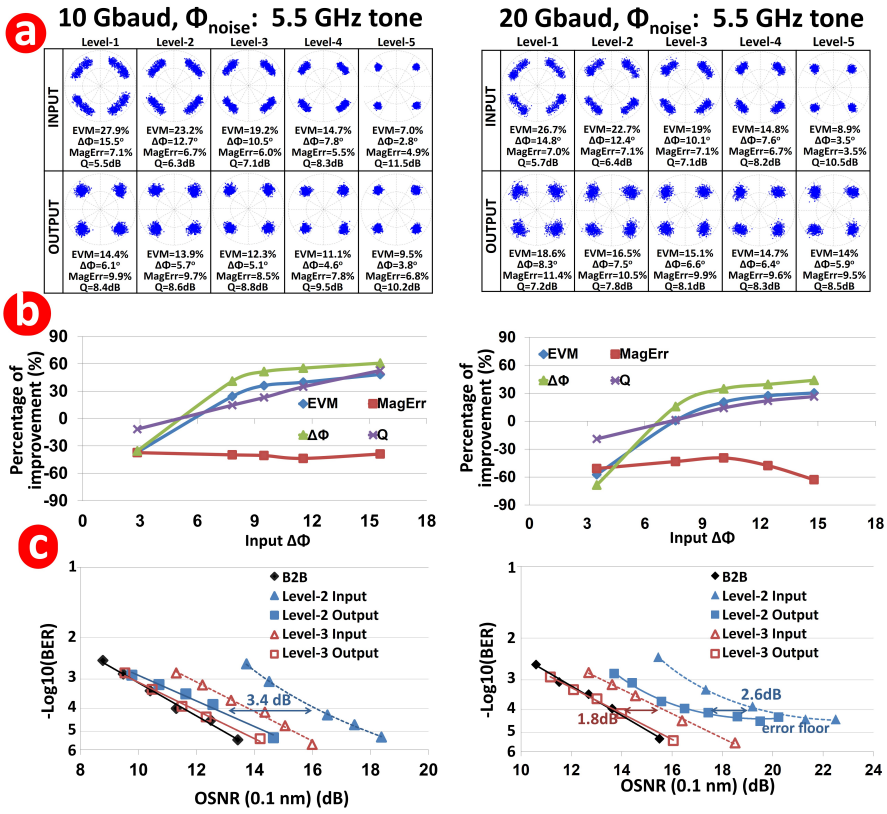

Fig. 4. (a) Constellations before and after the phase quantization system at various ϕ_{noise} levels. (b) Percentages of improvement in the figures-of-merit corresponding to input phase noise variance ($\Delta\Phi$) levels. (c) BER performance of the quantization system.

Next, we tune the system and examine the quantization performance for a 10-Gbaud QPSK with Level-2. In Fig. 5(a), the phase of the amplified idler$_{4\phi_S}$ is tuned using the LCoS filter, and the output EVM exceeds the input EVM (23.3%) after 60° of phase tuning. The BA pump is then frequency-shifted from the optimal ν_B and the phase quantization performance is recorded in Fig. 5(b). Results in Fig. 5(b) show that EVM exceeds the input EVM level of 23.3% after ~3 MHz of BA-pump frequency tuning.

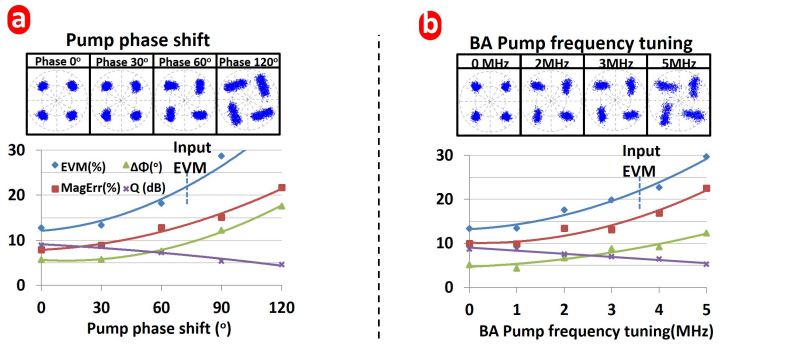

Fig. 5. (a) Impact of tuning the phase of idler$_{4\phi_S}$ on the phase quantization system. (b) Effect of tuning the frequency shifter of the BA on the quantized output.

Afterwards, the phase-locking behavior of the phase quantization system is examined over time. Figure 6(a) shows the histogram of input and the phase quantized output at 10 Gbaud with ϕ_{noise} of Level-3. Fig. 6(b,c) characterizes the performance over an hour without phase adjustments or a PLL, using the EVM and $\Delta\phi$ as figures-of-merit. Results indicate that the output started operating around EVM of 15%, but abrupt degradation happened after 36 minutes. This degradation is caused by bias drifting of the MZM frequency shifter and the changes in the room temperature. The MZM should operate at the null but instead varied, because it was manually adjusted at the start and then left to run freely. Also, slight room-temperature variations cause degradation, because ν_{B} varies with 1 MHz per degree centigrade in the SMF-28 [12]. Once the MZM bias and ν_{B} are re-optimized, the system could return to operate as normal.

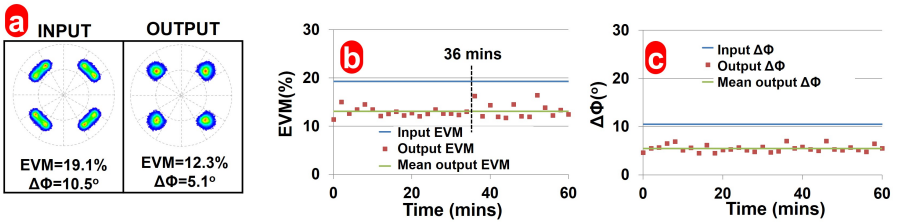

Fig. 6. (a) Histograms of input and phase quantized 10-Gbaud output signal. (b,c) Free-running stability test over an hour without a PLL. The performance is characterized by (b) EVM and (c) $\Delta\phi$.

Finally, we replace the 5.5-GHz source driving the phase modulator with

white noise generated by an amplified-spontaneous emission (ASE) source and a photodiode to emulate the broadband ϕ_{noise} that could be accumulated in optical fiber links. The spectrum of amplifying idler$_{4\phi_S}$ is shown in Fig. 7(a). The performance improvement for a 10-Gbaud signal is shown in Fig. 7(b), and Fig. 7(c) shows the BER performance for various ϕ_{noise} levels.

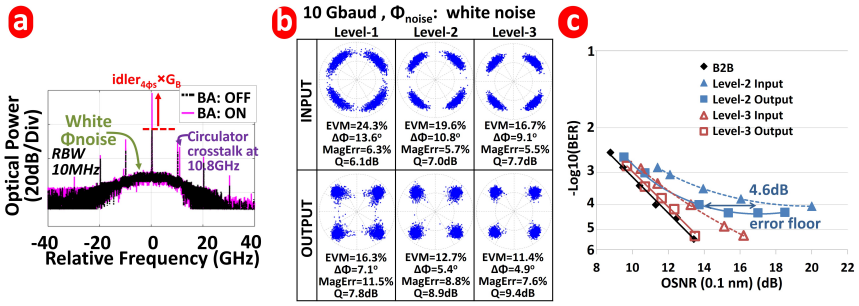

Fig. 7. (a) Spectrum of amplifying the central carrier of idler$_{4\phi_S}$ under the white noise case, captured using the 10-MHz OSA. (b) Constellations before and after the phase quantization system for a signal impacted with white ϕ_{noise}. (c) BER performance before and after the system.

6. Discussion and Conclusion

In conclusion, we experimentally demonstrated a phase-sensitive QPSK signal phase quantization system without an active phase-locked loop by amplifying the fourth-harmonic idler "in-line" using narrow bandwidth Brillouin amplification. The system performance under different baud rates and phase noise levels was investigated. We also evaluated the system sensitivity to various changing scenarios and showed stable phase quantization performance over 36 minutes without a PLL compared to a few seconds [5].

We believe our quantization system performance is limited by the final OSNR, and this can be improved by achieving better conversion efficiency in the HNLFs. For example, the improvement of conversion efficiency in HNLF$_1$ can result in creating idler$_{3\phi_S}$ with a higher power which can help to reduce the amount of loss applied to S for realizing the 10-dB power difference. Therefore, the overall OSNR after EDFA$_6$ can be increased.

The elimination of the active PLL for phase alignment between the pump, signal and idlers comes at the expense of adding Brillouin amplifier components. Although our system could operate without an active PLL over 36 minutes, actual system operation requires other means of feedback. For example, the system is polarization sensitive, and a polarization tracking system should be added. Also, Brillouin amplification is sensitive to the frequency-locking between the pump and probe. Thus, long-timescale feedback circuits to sense the temperature and tune the frequency shift accordingly might also be needed, which could be done using a frequency-locked loop (FLL) [15]. Finally, a conventional bias control circuit should be added to maintain the bias of the shifting MZM at the null.

In our experiment, we demonstrated quantizing only the phase states of a QPSK signal. However, an additional amplitude saturation stage could be added to reduce the amplitude noise as well [8, 16]. Also, future research could potentially investigate utilizing the gain saturation of Brillouin amplification [17] to reduce the amplitude noise on the fourth-harmonic idler.

7. Acknowledgments

The authors would like to acknowledge the support of Center for Integrated Access Network (CIAN) (Y501119); National Science Foundation (NSF) (ECCS-1202575); Defense Security Cooperation Agency (DSCA) (4440646262) and Fujitsu Laboratories of America (FLA).

8. References

[1] G. Li, Recent advances in coherent optical communication, Adv. Opt. Photon. 1 (2) (2009) 279–307. doi:10.1364/AOP.1.000279.

[2] G. Bosco, V. Curri, A. Carena, P. Poggiolini, F. Forghieri, On the performance of nyquist-WDM terabit superchannels based on PM-BPSK, PM-QPSK, PM-8QAM or PM-16QAM subcarriers, Journal of Lightwave Technology 29 (1) (2011) 53–61. doi:10.1109/JLT.2010.2091254.

[3] F. Parmigiani, R. Slavík, J. Kakande, P. Petropoulos, D. Richardson, Optical Regeneration, in: S. Wabnitz, B. Eggleton (Eds.), All-Optical Signal Processing, Springer International Publishing, 2015, pp. 129–155. doi:10.1007/978-3-319-14992-9_5.

[4] J. Kakande, R. Slavík, F. Parmigiani, A. Bogris, D. Syvridis, L. Grüner-Nielsen, R. Phelan, P. Petropoulos, D. J. Richardson, Multilevel quantization of optical phase in a novel coherent parametric mixer architecture, Nature Photonics 5 (12) (2011) 748–752. doi:10.1038/nphoton.2011.254.

[5] J. Kakande, A. Bogris, R. Slavk, F. Parmigiani, D. Syvridis, M. Skld, M. Westlund, P. Petropoulos, D. J. Richardson, QPSK phase and amplitude regeneration at 56 Gbaud in a novel idler-free non-degenerate phase sensitive amplifier, in: Optical Fiber Communication Conference and Exposition and the National Fiber Optic Engineers Conference, 2011. doi:10.1364/OFC.2011.OMT4.

[6] M. Asobe, T. Umeki, H. Takenouchi, Y. Miyamoto, In-line phase-sensitive amplification of QPSK signal using multiple quasi-phase matched LiNbO 3 waveguide, Optics Express 22 (2014) 26642. doi:10.1364/OE.22.026642.

[7] K. R. Bottrill, R. Kakarla, F. Parmigiani, D. Venkitesh, P. Petropoulos, Phase regeneration of QPSK signal in SOA using single-stage, wavelength converting PSA, IEEE Photonics Technology Letters 28 (2) (2016) 205–208. doi:10.1109/LPT.2015.2489843.

[8] A. Mohajerin-Ariaei, M. Ziyadi, M. R. Chitgarha, A. Almaiman, Y. Cao, B. Shamee, J. Yang, Y. Akasaka, M. Sekiya, S. Takasaka, R. Sugizaki, J. D. Touch, M. Tur, C. Langrock, M. M. Fejer, A. E. Willner, Phase noise mitigation of QPSK signal utilizing phase-locked multiplexing of signal harmonics and amplitude saturation, Optics Letters 40 (2015) 3328–3331. doi:10.1364/OL.40.003328.

[9] N. Kjøller, F. Da Ros, K. M. Røge, M. Galili, L. K. Oxenløwe, QPSK regeneration without active phase-locking, in: Conference on Lasers

and Electro-Optics, CLEO, Optical Society of America (OSA), 2016. doi:10.1364/CLEO_AT.2016.JTh2A.119.

[10] A. Almaiman, Y. Cao, M. Ziyadi, A. Mohajerin-Ariaei, P. Liao, C. Bao, F. Alishahi, A. Fallahpour, B. Shamee, N. Ahmed, A. J. Willner, Y. Akasaka, T. Ikeuchi, S. Takasaka, R. Sugizaki, S. Wilkinson, J. D. Touch, M. Tur, A. E. Willner, Experimental demonstration of phase-sensitive regeneration of a binary phase-shift keying channel without a phase-locked loop using Brillouin amplification, Optics Letters 41 (2016) 5434–5437. doi:10.1364/OL.41.005434.

[11] A. Almainman, Y. Cao, M. Ziyadi, A. Mohajerin-Ariaei, P. Liao, C. Bao, F. Alishahi, A. Fallahpour, B. Shamee, J. Touch, Y. Akasaka, T. Ikeuchi, S. Wilkinson, M. Tur, A. E. Willner, Experimental demonstration of phase-sensitive regeneration of a 20-40 Gb/s QPSK channel without phase-locked loop using Brillouin amplification, in: ECOC 2016; 42nd European Conference on Optical Communication, 2016.

[12] G. Agrawal, Nonlinear fiber opticsdoi:10.1016/B978-0-12-397023-7.00018-8.

[13] B. J. Eggleton, C. G. Poulton, R. Pant, Inducing and harnessing stimulated Brillouin scattering in photonic integrated circuits, Advances in Optics and Photonics 5 (4) (2013) 536. doi:10.1364/AOP.5.000536.

[14] W. Wei, L. Yi, Y. Jaouën, W. Hu, Bandwidth-tunable narrowband rectangular optical filter based on stimulated Brillouin scattering in optical fiber, Optics Express 22 (19) (2014) 23249. doi:10.1364/OE.22.023249.

[15] W. Khalil, S. Shashidharan, T. Copani, S. Chakraborty, S. Kiaei, B. Bakkaloglu, A 700-uA 405-MHz All-Digital Fractional-N Frequency-Locked Loop for ISM Band Application, IEEE Transactions on Microwave Theory and Techniques 59 (5) (2011) 1319–1326. doi:10.1109/TMTT.2011.2114897.

[16] K. R. H. Bottrill, G. Hesketh, L. Jones, F. Parmigiani, D. J. Richardson, P. Petropoulos, Full quadrature regeneration of QPSK signals using sequential phase sensitive amplification and parametric saturation, Optics Express 25 (2017) 696. doi:10.1364/OE.25.000696.

[17] L. Xing, L. Zhan, S. Luo, Y. Xia, High-power low-noise fiber brillouin amplifier for tunable slow-light delay buffer, IEEE Journal of Quantum Electronics 44 (12) (2008) 1133–1138. doi:10.1109/JQE.2008.2004601.